CrossMark

Exploiting the Balance Between Conductivity and Adsorption Capacity/Redox Electrocatalytic Ability In MIL-Based Porous Crystalline Materials for the Electrochemical Response

Tuyet Nhung Pham,[1,z] Xuan Nui Pham,[2] Hoa Thi Nguyen,[2] Thanh Pham,[2] Quang Huy Tran,[1] and Anh-Tuan Le[1,3,z]

[1]*Phenikaa University Nano Institute (PHENA), PHENIKAA University, Hanoi 12116, Vietnam*
[2]*Department of Chemical Engineering, Hanoi University of Mining and Geology, Duc Thang, Bac Tu Liem District, Hanoi, Vietnam*
[3]*Faculty of Materials Science and Engineering, PHENIKAA University, Hanoi 12116, Vietnam*

MIL-53(Fe), MIL-101(Cr), and MIL-53(Al) were successfully prepared and selected as promising modifying materials on electrode surface. With the difference in porous textural parameters and metal nodes, the physical characteristics, electrochemical behaviors, and performances towards chloramphenicol (CAP) detecting at each modified electrode were systematically evaluated through cyclic voltammetry (CV) and differential pulse voltammetry (DPV) measurements. Results pointed out that both MIL-53 (Fe)/SPE and MIL-101(Cr)/SPE exhibited excellent electrochemical performance through the enhancement of the EASA value, electrocatalytic ability, adsorption capacity (Γ), diffusion ability, and interaction with the CAP molecules, promising to be great materials in fabricating electrode. In which, MIL-101(Cr)/SPE with a huge BET, large pore volume, and good redox electrocatalytic ability of Cr^{3+} metal nodes significantly enhanced electrochemical response of CAP, despite it was still limited by poor adsorption capacity and diffusion due to the strong water-molecule interaction force of the Cr^{3+} centers and steric effect of the cramped microporous system. While, MIL-53(Fe) with a much smaller specific surface area and pore volume, it still showed good electrocatalytic activity of Fe^{3+} ions, along with high interact-ability and large adsorption capacity with CAP through hydrogen bonding and weak interaction force with water. In contrast, MIL-53(Al)/SPE showed poor electrochemical performance due to weak electron conductivity and the lack of electrocatalytic active sites. Obviously, in addition to conductivity, the merits of high adsorption capacity and excellent electrocatalytic activity of unsaturated metal centers need to be maximumly taken advantage of. A perfect balance in terms of the conductivity and adsorption capacity, as well as the electrocatalytic ability in MIL materials still needs to be further preferred in electrochemical sensors.
© 2022 The Electrochemical Society ("ECS"). Published on behalf of ECS by IOP Publishing Limited. [DOI: 10.1149/1945-7111/ac707b]

In recent years, MOF materials, especially the MIL family (MIL, Materials of Institute Lavoisier), are attracting more and more great interest from scientists in the field of electrochemical sensors for the detection of organic pollutants and different toxic compounds. Thanks to possessing many outstanding features arising from the unique self-assemblies of trivalent metal ions and terephthalate organic ligands such as highly porous crystalline material, stable ordered structures, adjustable pore size, large surface area, good absorbability, low cost, nontoxic nature, optical/optoelectronic nature, and especially excellent catalytic properties of metal nodes,[1–5] MIL porous crystalline materials have proved to be suitable factors to modify the electrode surface for improving the sensing performance. Among the MIL series, the MIL-53(Al), MIL-53(Fe), and MIL-101(Cr) are ones of representative materials with extensive attention to be catalysts in organic reactions, photocatalytic reactions, and even electrochemical reactions.[6–11] For instance, Cheng et al.[6] used MIL-53(Fe) to modify the glassy carbon electrode (GCE) surface for the effective electrochemical determination of the presence of H_2O_2 and NO_2^-. The obtained results exhibit that MIL-53(Fe)/GCE not only provided wider linear concentration ranges and lower detection limits but also showed an excellent anti-interference, reproduction, and stability, compared with the other modified electrodes. In another report, Li et al.[12] also introduced an electrocatalytic catalyst of MIL-101(Cr) towards the oxidation of dopamine and uric acid. The proposed material provided excellent performance and proved its great application potential in electrochemical sensors. Very recently, Meng and co-workers demonstrated the high application potential of MIL-53(Fe) in phenol electrochemical sensing. A novel composite based on Fe_2O_3/MIL-53(Fe)/rGO was fabricated and used to investigate the electrochemical behaviors of phenol. The proposed electrode exhibited a wide linear range, a low detection limit, as well as good reproducibility and stability.[13] Zhang et al.[14]

fabricated a MIL-101(Cr)/XC-72/GCE for the detection of chloramphenicol (CAP) in the various real samples (honey, eye drops, and milk) with satisfactory recoveries. Similarly, the MIL-53(NiFe)-based sensor showed good practicability for sensitive non-enzymatic glucose detection. Benefiting from the abundant active sites and its good stability in an alkaline solution, the MIL-53(NiFe)-based sensor exhibited high sensitivity and a low detection limit in the concentration linear range from 2 to 1600 μM.[15]

Clearly, most of these studies have shown positive effects on sensor performance and further confirmed the promising application potential of MIL materials in electrochemical applications. However, as a whole, they have just offered preliminary assessments by presenting and analyzing the enhancements recorded in terms of electrochemical response, selectivity, stability, and reproducibility in the electrodes modified with MIL materials. Detailed reports and in-depth analysis of the important effects of MIL on electrode characteristics in electrochemical reactions, in fact, have been still limited. From the structural perspective, as can be seen, both MIL-53(Al) and MIL-53(Fe) have the same formula as $M(OH)\{O_2C-C_6H_4-CO_2\}$ (M=Al or Fe).[1,16] Their three-dimensional frameworks are generally built up from corner-sharing chains of $M^{III}O_4(OH)_2$ octahedra interconnected through terephthalate groups, along with the formation of infinite one-dimensional linkage (–M–O–O–M–O–M–) to create a one-dimensional diamond-shaped pore system.[2] Meanwhile, for MIL-101(Cr), it is formulated as $Cr_3F(H_2O)_2O\{O_2C-C_6H_4-CO_2\}_3$. It is made of trimers of Cr^{3+} octahedra linked with terephthalate, forming supertetrahedral motifs that further assemble to produce crystallized porous hybrid architectures with huge surface areas.[16,17] According to that, both MIL-53(Al), MIL-53(Fe), and MIL-101(Cr) frameworks are semiconductor-like materials with many similar physical characteristics.[18] Ignoring the promising properties of MILs as mentioned, only their weak conductivity due to its rich organic linkers in crystalline structure also is a critical drawback, which directly inhibits their sensor applications.[19] Although, why did MIL-directly modified electrodes still exhibit impressive results in electrochemical sensing performance. In order to understand this phenomenon, researchers need to focus on the MIL's

[z]E-mail: nhung.phamthituyet@phenikaa-uni.edu.vn; tuan.leanh@phenikaa-uni.edu.vn

influence nature on the electrochemical behaviors over the modified electrodes. The aim of this work is therefore to assess whether or not the remarkable impacts of MIL materials on electrochemical behaviors and, if so, how it will be impacted? Namely, in this case, the electrochemical characteristics are electrical conductivity, adsorption capacity, and redox electrocatalytic ability including parameters: the active electrochemical surface area (AESA), adsorption capacity (Γ), diffusion ability, electrocatalytic activity in electrochemical reactions, and the interaction ability of the adsorbent with the electrode surface. Both MIL-53(Fe), MIL-101(Cr), and MIL-53(Al) were selected as the modifying materials, which had different porous textural parameters and structural components. The physical characteristics and electrochemical behaviors, as well as electrochemical performances in CAP detecting at each MIL-modified electrode were systematically evaluated through cyclic voltammetry (CV) and differential pulse voltammetry (DPV) measurements. In particular, MIL-53(Fe)/SPE and MIL-101 (Cr)/SPE exhibited excellent electrochemical performance towards CAP detection, promising potential materials in fabricating electrode. Meanwhile, MIL-53(Al)/SPE showed rather poor electrochemical performance. The important conclusion from this work is that exploiting a balance between the conductivity and adsorption capacity as well as the electrocatalytic ability of MIL materials is extremely important in electrochemical sensor applications. The MIL-modified electrodes are not necessarily too high conductivity for electron transfer, instead, the merits of adsorption capacity and electrocatalytic activity need to be maximumly taken advantage of. A high potential electrochemical material had to meet not only good conductivity but also in terms of both the high adsorption capacity and the electrocatalytic activity.

Experimental

Materials.—Hydrogen fluoride (HF, 48%), terephthalic acid (TPA), $Cr(NO_3)_3 \cdot 9H_2O$, dimethylformamide (DMF, >98%), ammonium fluoride (NH_4F, >96%), $Al(NO_3)_3$, $FeCl_3 \cdot 6H_2O$ were provided from Xilong Scientific Co., Ltd. and Guangdong Guanghua Sci-Tech Co., Ltd. Chloramphenicol (CAP) (>99% purity) was supplied by Sigma-Aldrich. $K_3Fe(CN)_6/K_4Fe(CN)_6$ (>99%) and ethanol (EtOH) were provided by Xilong Scientific Co., Ltd. PBS buffer (pH 7.4) was prepared using NaCl, KCl, $Na_2HPO_4 \cdot 12H_2O$, and KH_2PO_4 purchased from Merck KGaA, Germany, and Sigma-Aldrich. All chemicals used in this work were of reagent grade. In addition, the double-distilled water used in the whole experimental process was purified through a Milli-Q system (18.2 MΩ•cm at 25 °C). The commercial carbon screen-printed electrodes (SPEs-DS110) were supplied by DS Dropsens, Spain.

Methods

Synthesis of MIL-53(Fe), MIL-101(Cr), and MIL-53(Al).— *Synthesis of MIL-101(Cr).*—MIL-101(Cr) was prepared by the hydrothermal method in acid condition with the HF: TPA mole ratio of (0.25) as reported.[20–22] Briefly, a salt solution of 6.52 g $Cr(NO_3)_3 \cdot 9H_2O$ in 80 ml H_2O was added in as-prepared HF: TPA solution and stirred at room temperature for 3 h. This reacting mixture was then transferred to a Teflon-lined stainless-steel auto-clave to carry out the hydrothermal process at 200 °C for 9 h. After cooled down to room temperature, the mixture was washed thoroughly with DMF at 100 °C for 3 h, ethanol at 80 °C for 24 h, and then NH_4F 1 M solvent at 70 °C for 24 h. Finally, the solid product was collected, washed with H_2O, and dried under 100 °C for 24 h. The green solid was labeled by MIL-101(Cr).

Synthesis of MIL-53(Al).—A mixture of 2.6 g $Al(NO_3)_3$ and 0.576 g TPA was prepared in 100 ml DI-water and stirred at room temperature for 3 h. It was then transferred to a Teflon-lined stainless-steel autoclave and heated to 220 °C. The white solid was separated through centrifugation and decantation. It was washed three times with DI-water and finally dried overnight at 80 °C.[23,24]

Synthesis of MIL-53(Fe).—MIL-53(Fe) was synthesized by the hydrothermal method.[25,26] Firstly, a reacting mixture of 1.35 g $FeCl_3 \cdot 6H_2O$ and 0.83 g TPA was prepared in 25 ml of DMF solvent and stirred at room temperature for 30 min. This mixture was then transferred to a Teflon-lined stainless-steel autoclave and heated to 150 °C for 15 h. After cooling down to room temperature, the precipitate was separated and dried at 60 °C for 12 h. Finally, the solid product was re-dispersed in ethanol and H_2O to remove residue DMF. The yellow solid was dried and labeled MIL-53(Fe).

Preparation of MIL-53(Fe)–, MIL-101(Cr)–, and MIL-53(Al)-Modified SPE.—The modification of the working electrode surface with various MIL materials was carried out by a facile dropping method. Firstly, the commercial SPE was washed several times with ethanol and dried at room temperature. 10 mg of the synthesized MIL material was added into 10 ml double-distilled water, then sonicated for 30 min to create homogeneous suspensions. 6 μl of each above suspension was carefully dropped cast onto the working electrode surface, respectively. After drying naturally, the modified electrodes were still maintained in the dry air before using them for the next electrochemical measurements.

Characterizations.—The morphology and size of the synthesized MIL materials were observed via transmission electron microscopy (TEM) images using a JEOL JEM 1010-TEM system. The X-ray diffraction (XRD) patterns were used to study structural characterizations on the Bruker D5005 X-ray diffractometer with Cu Kα radiation (l = 1.54 Å). Fourier transform infrared spectroscopy (FTIR) measurements were recorded on a IRAffinity-1S spectrometer to provide information about functional groups on the MIL material surface. In addition, the pH values in the whole experimental process were adjusted by an IC-PH60 pH tester kit.

Evaluation of electrochemical characterizations.—To investigate the electrochemical characterizations of all bare or modified electrodes in this work, electrochemical measurements were carried out on a Palmsens 4 electrochemical workstation (PS Trace-Netherlands), a three-electrode system, at room temperature. The cyclic voltammetry (CV) measurements in the potential range from −0.3 to 0.6 V at a scan rate of 50 mV s^{-1} were performed using 0.1 M KCl solution containing 2.5 mM $K_3[Fe(CN)_6]/K_4[Fe(CN)_6]$ as a redox probe. Also, the electrochemical impedance spectroscopy (EIS) measurements were carried out in the frequency range from 0.01 to 50000 Hz at the different modified electrodes. Furthermore, the electrochemical performance of CAP on the bare SPE and modified SPEs was evaluated through CV and differential pulse voltammetry (DPV) measurements using a 0.1 M PBS buffer as the supporting electrolyte. In which, CV measurements were carried out at a scan rate of 50 mV s^{-1} in the potential range from −1.1 to 0 V. Also, DPV measurements were done at the following conditions: scan rate of 6 mV s^{-1}, E_{pulse} = 0.075 V, T_{pulse} = 0.2 s, and $T_{equilibrium}$ = 120 s.

Results and Discussion

Physical characterizations.—To demonstrate the successful synthesis of crystallographic MIL structures, XRD measurements for MIL-53(Al), MIL-53(Fe), and MIL-101(Cr) were carried out as illustrated in Fig. 1a. As can be seen, the XRD diffraction pattern of MIL-53(Al) showed sharp and strong peaks at about $2\theta = 9.4°$, 10.25°, 15.57°, 18.6°, and 21.3°, which were consistent with that of the simulated MIL-53(Al).[1,3,27] The XRD pattern of the as-synthesized MIL-101(Cr) also clearly exhibited the characteristic diffraction peaks at 2 angles of 3.3°, 5.1°, 8.4°, 9.1°, and 16.7°, which were essentially the same as those of the MIL-101(Cr) reported in Refs. 14, 28. Besides, for MIL-53(Fe), the presence of peaks located at 2θ = 9.4°, 11.2°, 12.7°, 17.8°, 22.3°, and 25.6° matched well with the diffraction data reported for MIL-53(Fe) in literature,[2,10,29,30] demonstrating the successful synthesis of MIL-53(Fe) structure.
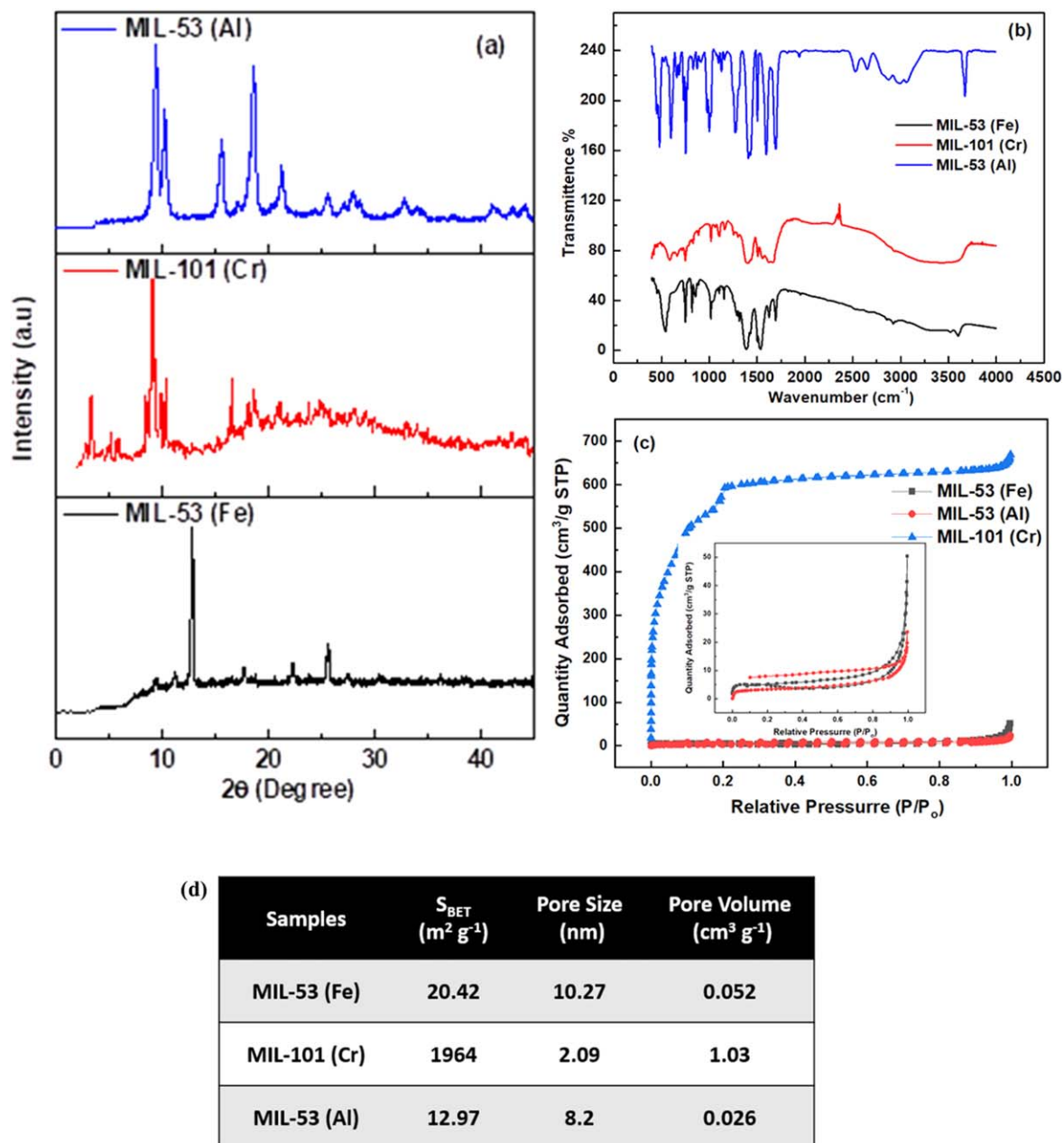
Figure 1. (a): XRD patterns, (b): FT-IR spectra, (c): Isotherm curves, and (d): Porous textural parameters of: MIL-53 (Fe), MIL-101 (Cr), and MIL-53 (Al).

Notably, in all three MIL materials proposed, no impurity phase was detected, indicating that these MIL structures were synthesized with high purity.

Besides, the molecular structure of the different MIL materials was verified by using FT-IR (see Fig. 1b). Especially, the infrared absorption spectra of MIL structures were in close agreement with the previous literature reports. Namely, the broad characteristic absorption peak at $3000 \, cm^{-1}$ was observed in both three MIL materials, suggesting the presence of hydroxyl groups (the O–H stretching vibration) arising from the water molecules adsorbed on the surface of MILs as well as the connection of 2-hydroxyter-ephthalic acid linkers.[1,2] Besides, the absorption peaks that appeared at 745 and $536 \, cm^{-1}$ were attributed to the C–H bonding vibrations of the benzene ring and the formation of a metal-oxo bond between the carboxylic group of TPA and metal (III) cations in the spectra of all three MILs structures.[2,6,18] In addition, the appearance of the two sharp absorption peaks at about 1400 and $1530 \, cm^{-1}$ was attributed to the symmetric and asymmetric stretching vibration of the C–O

bond of carboxylate groups, respectively.[1,2,6,18] Clearly, all the obtained evidence in the FT-IR spectra further demonstrated the effective formation of MILs structures.

To further study the important physicochemical characterizations of MIL materials, N_2 adsorption-desorption isotherm, pore size distribution, and porous textural parameters of both three MIL materials were presented in Figs. 1c and 1d, respectively. According to the IUPAC recommendation, both the two isotherms of MIL-53 (Al) and MIL-53(Fe) displayed a mode of the type-IV isotherm, corresponding to the dominant existence of mesoporous cages. Meanwhile, MIL-101(Cr) showed a higher N_2 adsorption capacity and the isotherm fitted well to type I, indicating the presence of abundant micropores in its crystal structure. According to the N_2 adsorption data, the specific surface area, total pore volume, and mean pore diameter for each MIL material were determined by the BET method as described in Fig. 1d, respectively. In which, MIL-101(Cr) achieved the highest values of the surface area of 1964 m^2 g^{-1} and total pore volume of 1.03 m^3 g^{-1} with a pore diameter of

2.09 nm. With these unique features, MIL materials, especially MIL-101(Cr) promise to offer many positive signals in electrochemical reactions of CAP for sensor applications.

The morphological properties and size of MIL structures were also observed by TEM images. As depicted in Fig. 2, each various MIL crystallized structure indicated different shapes and sizes. Indeed, for the MIL-53(Fe) image, it showed a well-crystallized rod-like structure with a size in the nanoscale of around 60–80 nm in diameter, while, the prepared MIL-101(Cr) looked like highly ordered hexahedral particles with an average size of about 1.5 μm. Figure 2c displayed the TEM images of MIL-53(Fe) with a special microstructure and morphology of the uniform rod-shaped particles, gathering together, and most of the particles' size of bout 20–40 nm in diameter.

Electrochemical investigations.—For the first investigation of the electrochemical properties of modified electrodes, CV measurements were carried out in 0.1 M KCl containing 5 mM $Fe(CN)_6^{3-/4-}$ at a scan rate of 50 mV s^{-1} described in Fig. 3a. The pair of reversible redox peaks, which is attributed to the electron transfer between Fe^{2+} and Fe^{3+}, was observed at the potential range from -0.3 to 0.6 V for all MIL-modified electrodes and even bare SPE. More interestingly, there was a significant difference recorded in the redox peak current response. Namely, compared to the bare SPE, the MIL-53(Fe)/SPE, MIL-53(Al)/SPE, and MIL-101(Cr)/SPE exhibited an increase in ΔI_p value at both reduction $\Delta I_p(red)$ and oxidation $\Delta I_p(oxi)$ peaks, corresponding to about 174.7 μA for MIL-53(Al)/SPE, 174.5 μA for MIL-53(Fe)/SPE, and 158.3 μA for MIL-101(Cr)/SPE, respectively. To further understand this improvement, the

peak potential separation (ΔE_p) value, the active electrochemical surface area (AESA), and the resistance of charge transfer (R_{ct}) at high-frequency semicircle region in the Nyquist plot (Fig. 3c) were also determined for each modified electrode. In which, ΔE_p value tended to increase in the following order: bare SPE (199.6 mV) < MIL-53(Al)/SPE (201.8 mV) < MIL-53(Fe)/SPE (213 mV) < MIL-101(Cr)/SPE (214.5 mV). As we know, the ΔE_p value reflects the electron transferability in the electrochemical reactions of the $Fe(CN)_6^{3-/4-}$.[31] In this case, it decreased at all the MIL-modified electrodes, suggesting that the MIL materials effectively promoted the electron transfer on the modified electrodes. Although, the peak-to-peak potential separation and large deviation compared to its theoretical value of zero could be explained via critical proof of the inherent weak conductivity of organic linkers within these various MIL material structures. Besides, it could arise from the side chemical interactions between the electrolyte ions and the electrode, dominance of electrostatic factors, and even due to the presence of unwanted reactions on the electrode surface. This enhancement was further demonstrated by observing the obtained Nyquist diagrams in EIS measurements. Indeed, it can be seen that the largest well-defined semicircle at the high frequencies was recorded at the bare SPE, indicating large interface impedance and poor electrocatalytic activity. While the R_{ct} of the MIL-modified electrodes was much smaller, confirming the impressive promotion of electron transfer at MIL materials. Furthermore, Fig. 4 displays CV curves were recorded on the modified electrodes at the various scan rates of MIL-53(Fe)/SPE (a), MIL-101(Cr)/SPE (b), and MIL-53(Al)/SPE (c) in $[Fe(CN)_6]^{3-/4-}$/KCl aiming to investigate the effect of scan rate on the electron transfer characteristics. By varying scan rate
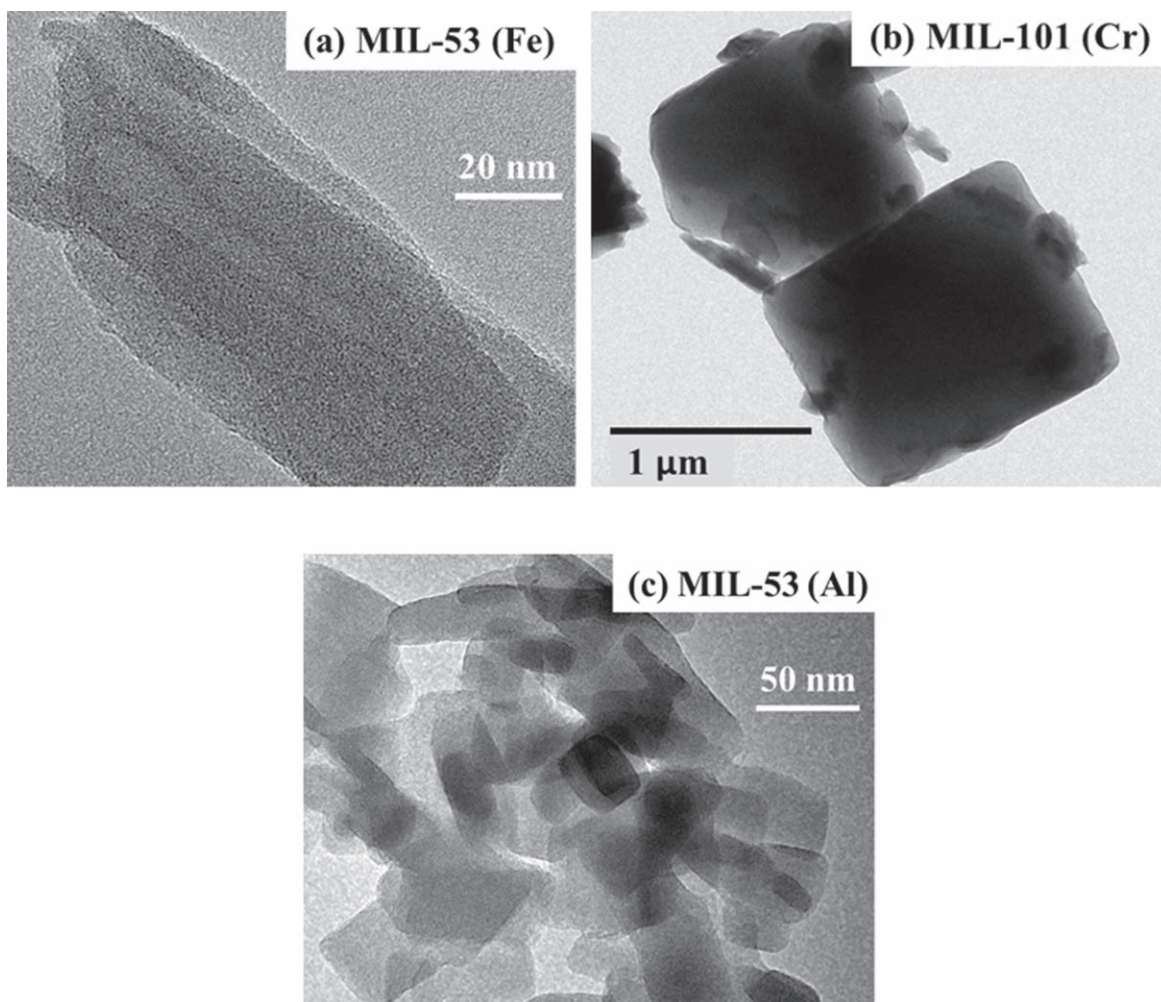

Figure 2. TEM images of (a): MIL-53(Fe); (b): MIL-101(Cr); and (c): MIL-53(Al).
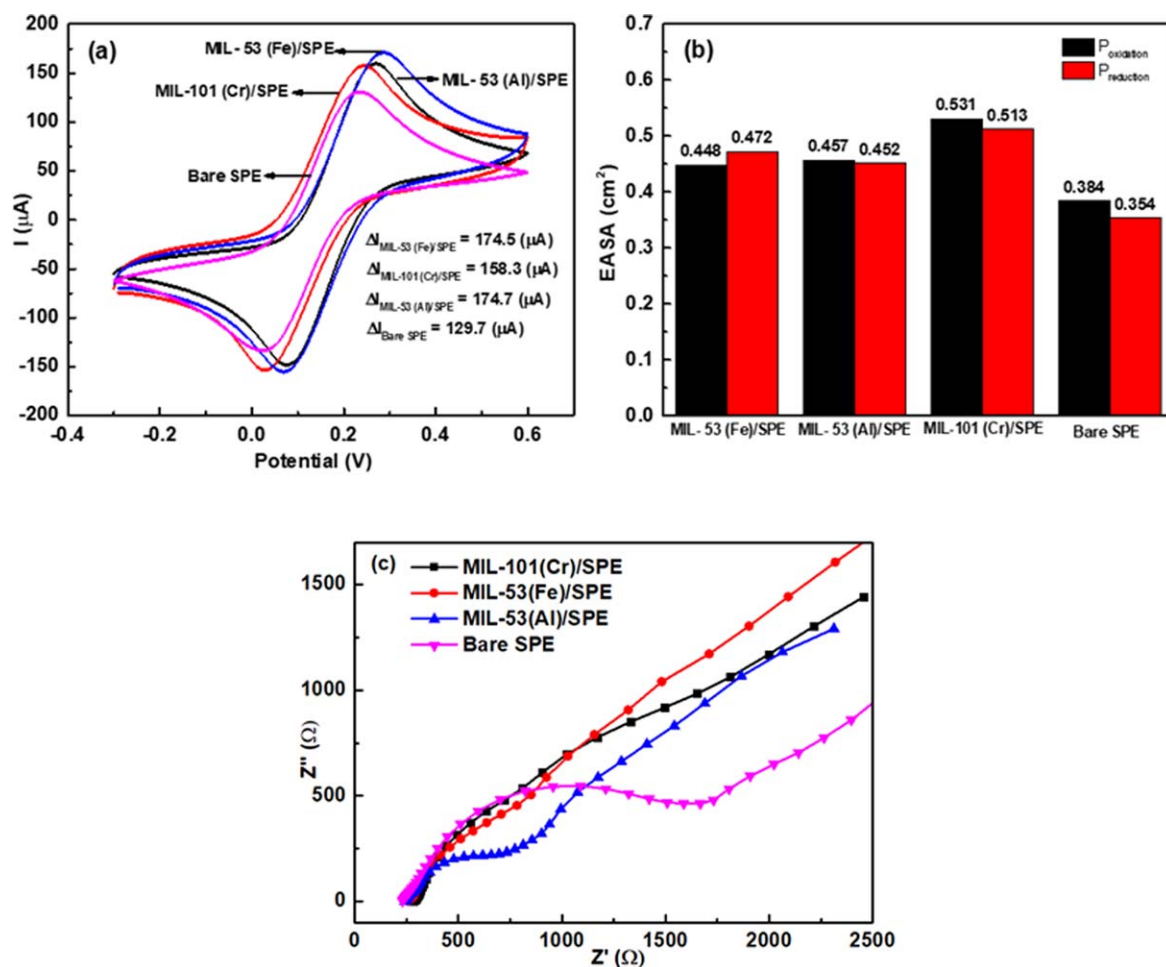
Figure 3. (a) and (c): a comparison of current response obtained from CV measurements and EIS results on various electrodes: MIL-53(Fe)/SPE, MIL-53(Al)/SPE, MIL-101(Cr)/SPE, and bare SPE in 0.1 M KCl containing 5 mM $Fe(CN)_6^{3-/4-}$; (b): the EASA calculated on various electrodes via ΔI_p(red) and ΔI_p(oxi).

from low (10 mV s^{-1}) to high (70 mV s^{-1}), the variation in the peak current value and slight shift in the redox peak potential value were observed. The linear responses were obtained in Figs. 4a'–4c' between ΔI_p value and square root of the scan rate, reflecting a complete diffusion-controlled process for the reversible electron transfer reaction of redox probe molecules over the modified electrodes.[32] From the obtained slope values of these plots, the AESA of each modified electrode could be calculated using the Randles-Sevcik equation (25 °C):

$$I_p = 2.69 \times 10^5 n^{3/2} A D^{1/2} \nu^{1/2} C$$

where n = 1 (number of electrons transferred in the redox reactions), A is AESA value (cm^2), D = 6.5 × 10^{-6} cm^2 s^{-1} (diffusion coefficient of Fe^{2+}/Fe^{3+} in 0.1 M KCl), ν is the scan rate, and C is the bulk concentration of redox probes. According to that, the A values for bare SPE, MIL-53(Fe)/SPE, MIL-53(Al)/SPE, and MIL-101(Cr)/SPE were determined of approximately 0.384, 0.448, 0.457, and 0.531 cm^2 as illustrated in Fig. 3b. In contrast with ΔE_p values, the AESA values of the modified electrodes were, in fact, remarkably improved, compared with that of bare SPE. This result is consistent with the unique characteristics of MIL materials when possessing a huge pore volume and high surface area as discussed in the above section.

From these obtained results, it shows that the electrode modification with MIL materials offered positive enhancements in terms of active electrochemical surface area and electron transfer. Unfortunately, their inherent poor electronic conductivity also led to sluggish charge-transfer kinetic at the modified electrodes.

Although, as we know, the charge-transfer kinetic is one of the important factors, which decides the electrochemical property of a modified electrode. However, in this case, why did the MIL-modified electrodes with slower charge-transfer kinetic still display the higher redox peak current response of the probe molecules, compared with bare SPE? It was essential to ascertain whether the nature of the increase in surface area herein was the main cause for this improvement. And, what are the critical impacts of MIL material in the electrode? These contents were investigated and discussed in detail in the next sections.

Electrochemical behaviors of CAP on modified electrodes.—To explore the electrochemical behaviors of CAP on the modified electrodes, CV measurements were carried out. As illustrated in Fig. 5a, no redox peak was observed in the CV curve with the absence of CAP, while a distinct reduction peak at the potential range of −0.7 V and a pair of slight redox peaks at around −0.2 V were recorded on the different modified electrodes and even bare SPE in 0.1 M PBS (pH-7.4) containing 50 μM CAP. However, the CV current response and peak potential value were varied at each modified electrode. Namely, the bare SPE showed a very weak electrochemical reduction signal of about 1.68 μA located at −0.7 V. On the contrary, by the electrode modification with MIL materials, the electrochemical response of CAP on the MIL-53(Fe)/SPE and MIL-101(Cr)/SPE was remarkably enhanced. The characteristic reduction current intensity was recorded at approximately 4.525 and 5.049 μA for MIL-53(Fe)/SPE and MIL-101(Cr)/SPE, which were 2.7− and 3-fold larger than bare SPE, respectively. Compared to other modified electrodes, MIL-53(Al)/SPE still exhibited a rather
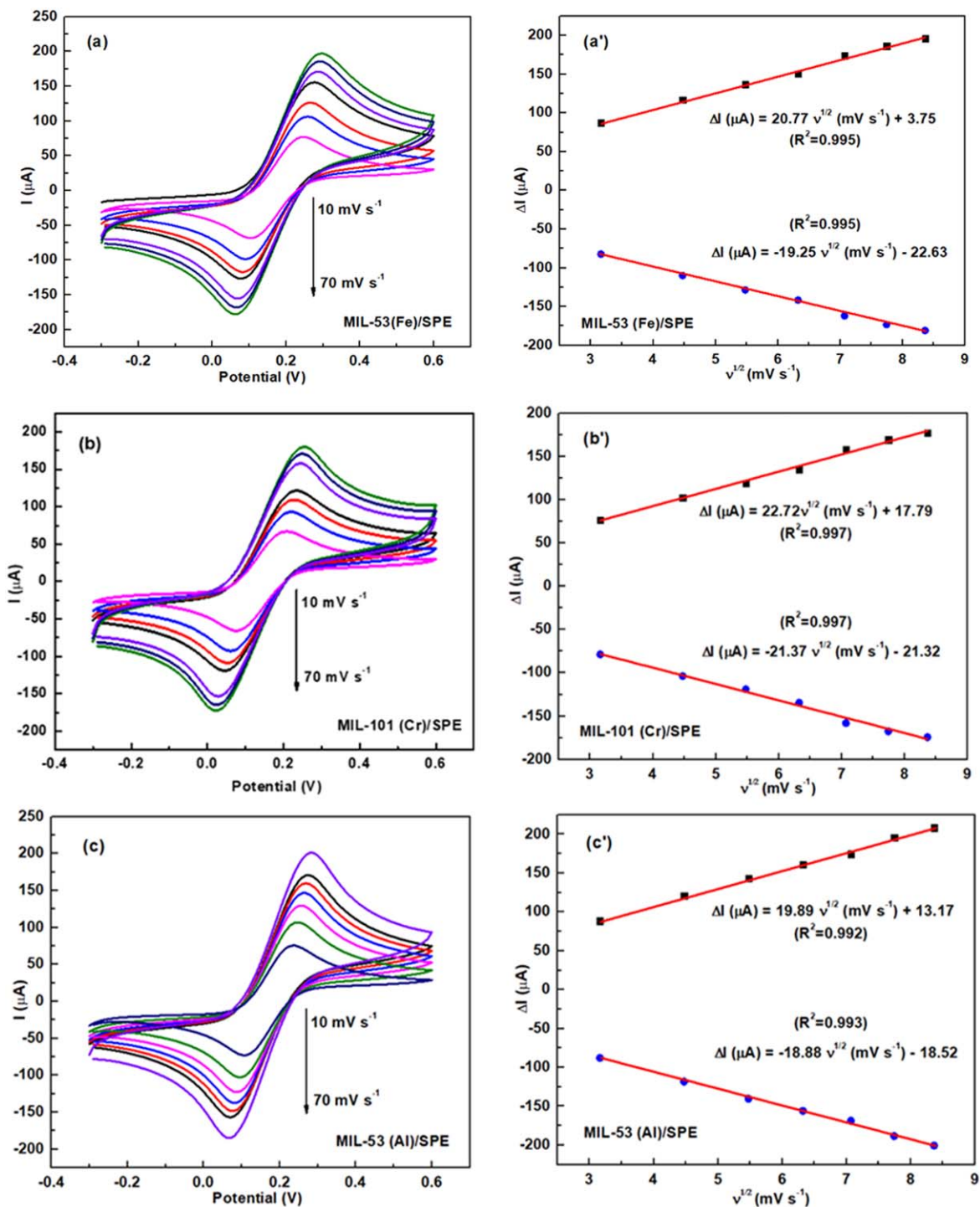
Figure 4. (a), (b), and (c): CV recorded on modified electrodes at various scan rates (10–70 mV s^{-1}), corresponding to the linear plots of oxidation and reduction peak current responses vs $\nu^{1/2}$ with error bars (a'), (b), and (c') in 0.1 M KCl containing 5 mM [Fe(CN)$_6$]$^{3-/4-}$.

weak reduction current of 2.018 μA. This improvement trend was also found in the results obtained from DPV measurements (Fig. 5b). According to that, the reduction current increased in the order: bare SPE (3.080 μA) < MIL-53(Al)/SPE (3.541 μA) < MIL-53(Fe)/SPE (8.353 μA) < MIL-101(Cr)/SPE (10.409 μA). On the other hand, when comparing the reduction peak potential value, it seems to the reduction reaction of CAP occurred at the more negative potential range on all the modified electrodes. Clearly, these results matched well the results from the electrochemical behaviors of Fe^{2+}/Fe^{3+} redox probes.

To explain these phenomena, it should be focused on the unique features in terms of the flexible three-dimensional structure and tunable composition of MIL materials. Firstly, benefiting from the flexible three-dimensional structure, the proposed MIL materials provided large porosity, uniform pore size, high specific surface area, and high chemical stability. These unique features contributed to the increase in AESA value of the modified electrodes, leading to the significant improvement in the electrochemical current response of both Fe^{2+}/Fe^{3+} probes and CAP molecules. With the possessing average pore diameter of > 2 nm in both three MIL-structures
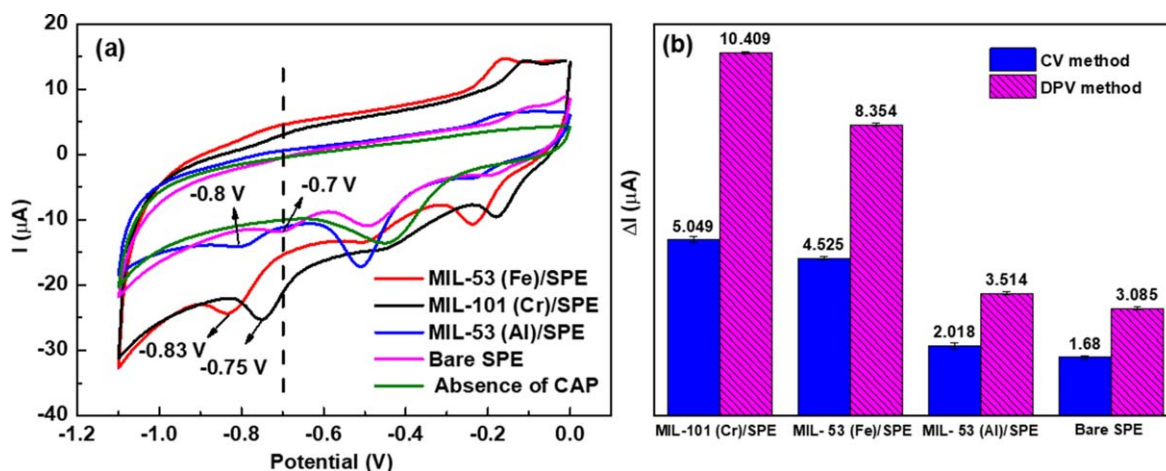
Figure 5. (a): CV profiles of various electrodes at a scan rate 50 mV s^{-1} in 0.1 M PBS (pH-7.4) containing 50 μM CAP and (b): Current responses recorded on various electrodes via CV and DPV measurements.

proposed, which was larger about 1.7 times than the geometry structure of the CAP molecule (3.93 × 8.30 × 11.03 Å, calculated using Gaussian 09 software),[33,34] it facilitated the CAP diffusion and adsorption process, that could happen inside the internal pores/channels of MIL materials through the "*pore effect*." More interestingly, in a correlation comparison between porous textural parameters (S_{BET} and pore volume) and the improvement of AESA value as well as the current response of CAP recorded, S_{BET} and pore volume of MIL-101(Cr) were 151 and 40-fold larger than those of MIL-53(Al) and 96 and 20-fold larger than those of MIL-53(Fe), but the AESA value and current intensity of MIL-101(Cr) were just larger around 1.16 and 2.96 times than those of MIL-53(Al) and around 1.18 and 1.24 times than those of MIL-53(Fe). From that, it seems to the huge surface area and large pore volume of MIL-101 (Cr) materials did not provide impressive improvements as expected, and therefore, it was not the only factor affecting the electrochemical activity on the MIL-modified electrodes.

Indeed, as mentioned in the introduction section, when considering the MIL's composition perspective, the presence of organic linkers in MIL structure, in fact, is a major cause leading to their sluggish electron and charge transferability. Meanwhile, inorganic metal clusters or coordination centers are considered as factors determining their geometries and physicochemical properties. Herein, the negative influence of MIL on the electron and charge transferability was pointed out in the shift towards a more negative potential direction of the CAP reduction peaks as well as the increase in the peak potential separation (ΔE_p). Furthermore, on the basis of the difference of metal centers and crystal structural geometries among the proposed MIL structures, it can see that MIL-53 (Fe) and MIL−101 (Cr) possessed a large density of unsaturated metal sites of Fe^{3+} and Cr^{3+} ions, respectively. Normally, these cations are able to electrocatalytic activity in electrochemical reactions owing to existing in variable oxidation states as well as the existence of the incompletely filled *d*-orbitals (Fe^{3+} = [Ar]3d^5) or empty *d*-orbitals (Cr^{3+} = [Ar]3d^{3+}). Indeed, the presence of such *d*-orbitals could support the electron acceptance or donation from the CAP molecules aiming to form the reduction or oxidation states and then exchange these electrons with the electrode surface to recover the initial state. So, these electrocatalytic activity sites facilitated the redox reactions of CAP to take place more easily and effectively on the MIL-modified electrode surfaces. Unfortunately, MIL-53(Al) material did not have these properties (Al^{3+} = [He]). The important influence of metal cations was further confirmed when considering the correlation relationship of the porous textural parameters and the improvement of AESA value as well as the current response of CAP between MIL-53(Fe) and MIL-53(Al). It should be stressed that, under the same crystal structural geometry, MIL-53(Fe) and MIL-53

(Al) exhibited similar porous textural parameters and a small difference in AESA value, however, the electrochemical current response obtained on the MIL-53(Fe)/SPE displayed a large difference of approximately 2.4 times in DPV measurements. Clearly, this comparison indicates that the existence of unsaturated metal active sites as having potential electrocatalytic activity in MIL-53(Fe) and MIL−101(Cr) was extremely important, thus it could be considered as a major factor that helped them remarkably enhance electrocatalytic activity in electrochemical sensing applications towards CAP detection.

It is known that the effect of scan rate on the electrochemical behaviors such as current intensity or peak potential position reflects the redox reaction dynamic of the targeted analyte. In this case, the effect of scan rate on the electrochemical behaviors of CAP at MIL-53(Fe)/SPE and MIL-101(Cr)/SPE was also evaluated via CV measurements in 0.1 M PBS containing 50 μM of CAP, respectively. As showed Fig. 6, by varying scan rate in the range from 10 to 70 mV s^{-1}, the cathodic peak currents recorded at both two modified electrodes linearly increased with the increase in scan rate, corresponding with linear regression equations: I_{pc} (μA) = -0.288 ν (mV s^{-1}) $- 7.158$ (R^2 = 0.997) for MIL-53(Fe)/SPE and I_{pc} (μA) = -0.259 ν (mV s^{-1}) $- 9.269$ (R^2 = 0.999) for MIL-101(Cr)/SPE, respectively. According to that, the redox process of CAP on these modified electrodes was the typical surface adsorption-controlled process. More importantly, based on these linear relationships, the adsorption capacity of CAP on the MIL-53(Fe)/SPE and MIL-101 (Cr)/SPE surface was also determined through the following equation: i_p = $n^2F^2A\nu\Gamma/4RT$. Namely, the adsorption capacity (Γ) of CAP at MIL-101(Cr)/SPE was equal to about 3.74 × 10^{-8} mol cm^{-2}, which was higher than that of MIL-53(Fe)/SPE (3.65 × 10^{-8} mol cm^{-2}), suggesting higher adsorption capacity of CAP on the MIL-101(Cr)/SPE arising from its large surface area and pore volume. Furthermore, it was observed that there were slight shifts of reduction peak potential towards more negative values at higher scan rates, which was explained due to the formation of diffusion layer on electrode surface causing the transfer limitation of charge and electrons. Particularly, the correlation between the cathodic peak potentials (E_{pc}) and (ln ν) was determined in good linear relationships of E_{pc} (V) = -0.043 ln (ν) (mV s^{-1}) $- 0.653$ (R^2 = 0.996) for MIL-53(Fe)/SPE and E_{pc} (V) = -0.039 ln (ν) (mV s^{-1}) $- 0.616$ (R^2 = 0.998) for MIL-101(Cr)/SPE, respectively.

The slight difference in calculation of adsorption capacity (Γ) and reduction current response (I_{pc}) of CAP is the best clear proof of the different electrocatalyst efficiency between the MIL-53(Fe) and MIL-101(Cr) structures used in the modification of the bare SPEs. Returning to the material characteristics of MIL-53(Fe) and MIL-101(Cr), both of them are not only porous typical materials but also
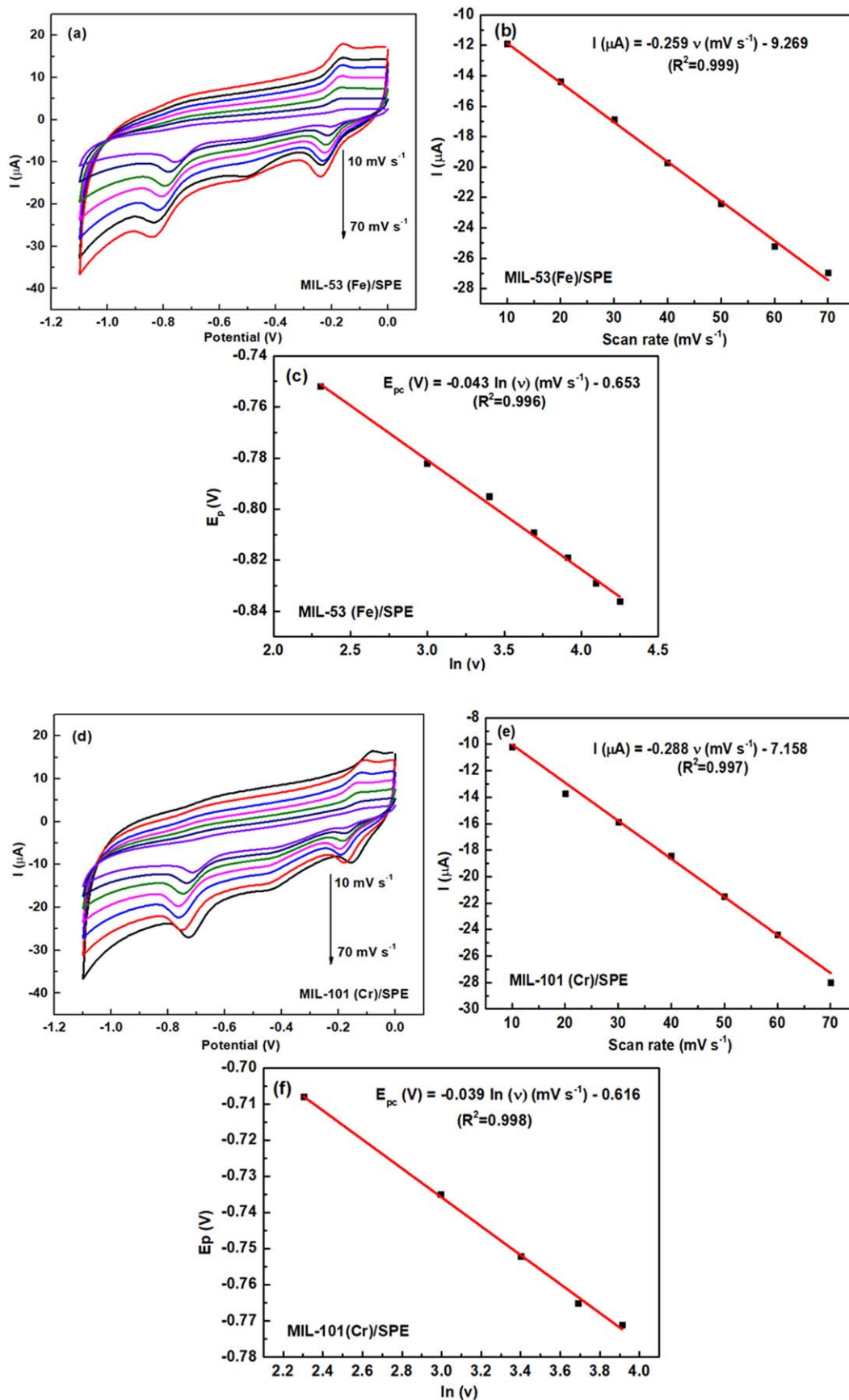
Figure 6. (a) and (d) CV responses recorded of 50 μM CAP in 0.1 M PBS (pH-7.4) on MIL-53(Fe)/SPE and MIL-101(Cr)/SPE; (b) and (c): The calibration plots of cathodic peak current (I_{pc}) vs various scan rates from 10 to 70 mV s^{-1} plots with error bars; (d) and (f): The plots of reduction peak potentials (E_{pc}) verus ln (ν).

self-assembly structures possessing a large number of the electro-catalytic active sites. It needs to stress that although MIL-101(Cr) offered a huge surface area and outstanding pore volume with the microporous system, which was 96 and 20-fold larger than those of MIL-53(Fe), it just showed increasing approximately of 1.18, 1.24, and 1.03-fold in AESA value, current intensity, and adsorption capacity (Γ), compared with MIL-53 (Fe) as above discussed. It is clear upon consideration again of these obtained results that the electrochemical activities of MIL-53(Fe)/SPE and MIL-101(Cr)/SPE were still affected by other factors. Namely, in this case, other factors can be inferred by the physicochemical properties of unsaturated metal centers such as interaction energy with water, interaction mechanism, and steric effects of the pore space between MIL-materials and CAP molecules.

As a full description within Figs. 7a and 7b, the effect of accumulation time on the peak current intensity of CAP was studied in detail over MIL-53(Fe)/SPE and MIL-101(Cr)/SPE. After 120 s of accumulation time, the reduction current response achieved the maximum value on both two modified electrodes, therefore, it was considered sufficient time to achieve adsorption equilibrium on the electrode surface. To further inspect the adsorption kinetic over these electrodes, DPV measurements were taken place by varying concentrations of CAP (Fig. 8). As can see, there was a linear increase of current intensity recorded along with an increase in the CAP concentration in the range of 1 to 50 μM, indicating the adsorption process of CAP onto the electrodes follows the Langmuir isotherm model. According to that, the monolayer and homogeneous adsorption of CAP molecules occurred onto the electrode surface, and of course, the adsorption capacity of CAP could be limited by the number of adsorptive sites with uniform energy and interaction ability.[1,29]

Similar to some recent reports, it pointed out that the high adsorption capacity and rapid adsorption of MIL species in liquid-phase adsorption processes remarkably depended on the inherent nature of central metal ions, for example, acidity, redox properties, and interaction energy of water. Indeed, it was reported that the adsorption energy of water over the different central metal ions in MIL-materials were different in the order: $Fe^{3+} < Al^{3+} < Cr^{3+}$,[35] corresponding to the rate constants for the exchange of the water molecules decreased in the order: $Fe^{3+} > Al^{3+} \gg Cr^{3+}$.[36] In which, the binding energy for the water adsorption on MIL-100(Cr) was determined to be higher (94.7 kJ mol^{-1}) than that on MIL-100(Fe) (75.5–80 kJ mol^{-1}).[37,38] From these, it is proposed that the adsorption process of CAP molecules on MIL-53(Fe) occurred more easily due to the water molecules can be easily desorbed and replaced from the MIL-53(Fe)/SPE electrode surface, compared with that onto MIL-101(Cr)/SPE. It may be concluded that the central metal ions of MIL not only played a significant role in electrocatalytic activity but also contributed to deciding the performance of adsorption/separation of adsorbent molecules in the liquid-phase adsorption process.

Another important reason that can impact the adsorption capacity of CAP onto the MIL-modified electrodes is the presence of some specific interactions between the electrode surface and the CAP molecule. Besides pore-selective adsorption of MIL-materials, similar to the adsorption mechanism of some organic compounds studied, the monolayer and homogeneous adsorption of CAP molecules onto the electrode surface under the Langmuir isotherm model could base on electron donor-acceptor interactions between oxygen-atoms of the carbonyl group and the aromatic ring of the adsorbate, Van der Waals bonding, electrostatic interactions, $\pi-\pi$ interaction, dipolar interactions, and particularly, hydrogen bonding. In regards to the formation of hydrogen bonding, maybe benefiting from a large number of [Fe(OH)] groups within the structure, MIL-53(Fe) reached a higher adsorption capacity. In order to further demonstrate this identification, the effect of pH on the current response was investigated by varying pH from 3 to 11, because pH has significant influences on the physicochemical properties of not only the adsorbate but also functional groups on the electrode surface (Figs. 7c–7f). For MIL-53(Fe)/SPE, it can see that the current increased as the pH increased from 3 to 7. This is consistent because CAP is hydrolyzed at pH < 2 or pH > 8. At low pH conditions, hydrogen bonding could be produced between N–H, −OH, and −NO$_2$ groups in CAP and −OH and C=O groups on MIL-53(Fe). With increased pH, some functional groups on MIL-53 (Fe) were ionized, along with that a competitive adsorption between −OH and the unsaturated metal sites made gradually weak the hydrogen bonding between CAP and MIL-53(Fe), resulting in decreasing CAP adsorption capacity and electron transferability. In contrast, for MIL-101(Cr)/SPE, the current response tended to increase when pH increased, which is probably explained due to the steric effect of the monolayer adsorption of CAP molecules inside cramped microporous channels with limitations of the number of adsorption sites and small pore size on MIL-101(Cr). Indeed, at high pH, CAP molecules were hydrolyzed and fracted to form smaller species, which resulted in decreased steric effect of CAP molecules in cramped spaces of microporous systems and increased diffusion rate as well as increased CAP adsorption kinetic. More interestingly, the reduction peak potential (E_{pc}) of CAP also linearly shifted in the considered pH range, corresponding to regression equations: $E_{pc} = -0.015$ pH—0.567 ($R^2 = 0.994$) for MIL-53(Fe)/SPE and $E_{pc} = -0.014$ pH—0.39 for MIL-101(Cr)/SPE ($R^2 = 0.993$).

Returning to Fig. 8, under the optimal condition of pH and incubation time for the modified electrodes, DPV measurements at each different CAP concentration showed the perfect linear relationship of current intensity vs concentration. The regression equation and R^2 was calculated such as $I_{pc}(\mu A) = 0.163$ CAP (μM) + 0.155; $R^2 = 0.999$ for MIL-53(Fe)/SPE and I_{pc} (μA) = 0.264 CAP (μM) + 0.089; $R^2 = 0.996$ for MIL-101(Cr)/SPE, respectively. According to the slope value, the limit of detection (LOD) of the CAP of each electrode was determined of about 0.121 and 0.075 μM (S/N = 3), respectively. It, therefore, manifests that the proposed electrodes afforded good electrocatalytic activities with low LOD and a wide detection range.

To further study the practical application potential of MIL-53 (Fe)/SPE and MIL-101(Cr)/SPE, DPV measurements were utilized in the demonstration of high repeatability and good selectivity of MIL-53(Fe)/SPE and MIL-101(Cr)/SPE. Indeed, the favorable repeatability of the proposed sensors towards CAP detecting was observed after ten successive repeated DPV measurements in 0.1 M PBS (pH = 7.4) containing 50 μM CAP using the same electrode. As one can see from Figs. 9a and 9c, the peak current change was very small and the relative standard deviation (RSD) was calculated about 2.7 and 1.19% for MIL-53(Fe)/SPE and MIL-101(Cr)/SPE. In addition, the electrochemical response of CAP under the presence of a high concentration of various interfering compounds was recorded. No significant change in the detection of CAP was found by adding Co^{2+}, Ni^{2+}, Mn^{2+}, Fe^{2+}, and even organic substances such as ascorbic acid, glucose, and 4-nitrophenol, revealing high selectivity to the determination of CAP. In short, MIL-53(Fe) and MIL-101(Cr) are potential electrochemical catalysts for CAP detection with satisfied electrochemical properties for sensor applications (Figs. 9b and 9d).

From a more general perspective, it is clear that not all MIL materials have the suitable features to meet the requirements of potential material in sensing applications. Indeed, with MIL-53(Al), though it showed an increase in EASA, it was not enough to bring about a remarkable improvement in CAP detection performance due to poor electron conductivity and the lack of electrocatalytic active sites. In contrast, the electrodes modified with MIL-53(Fe) and MIL-101(Cr) showed positive signals in improving the electrochemical response of CAP through the enhancement of both EASA, electro-catalytic ability, adsorption capacity, diffusion ability, and interact ability with the CAP molecules. More namely, MIL-101(Cr)
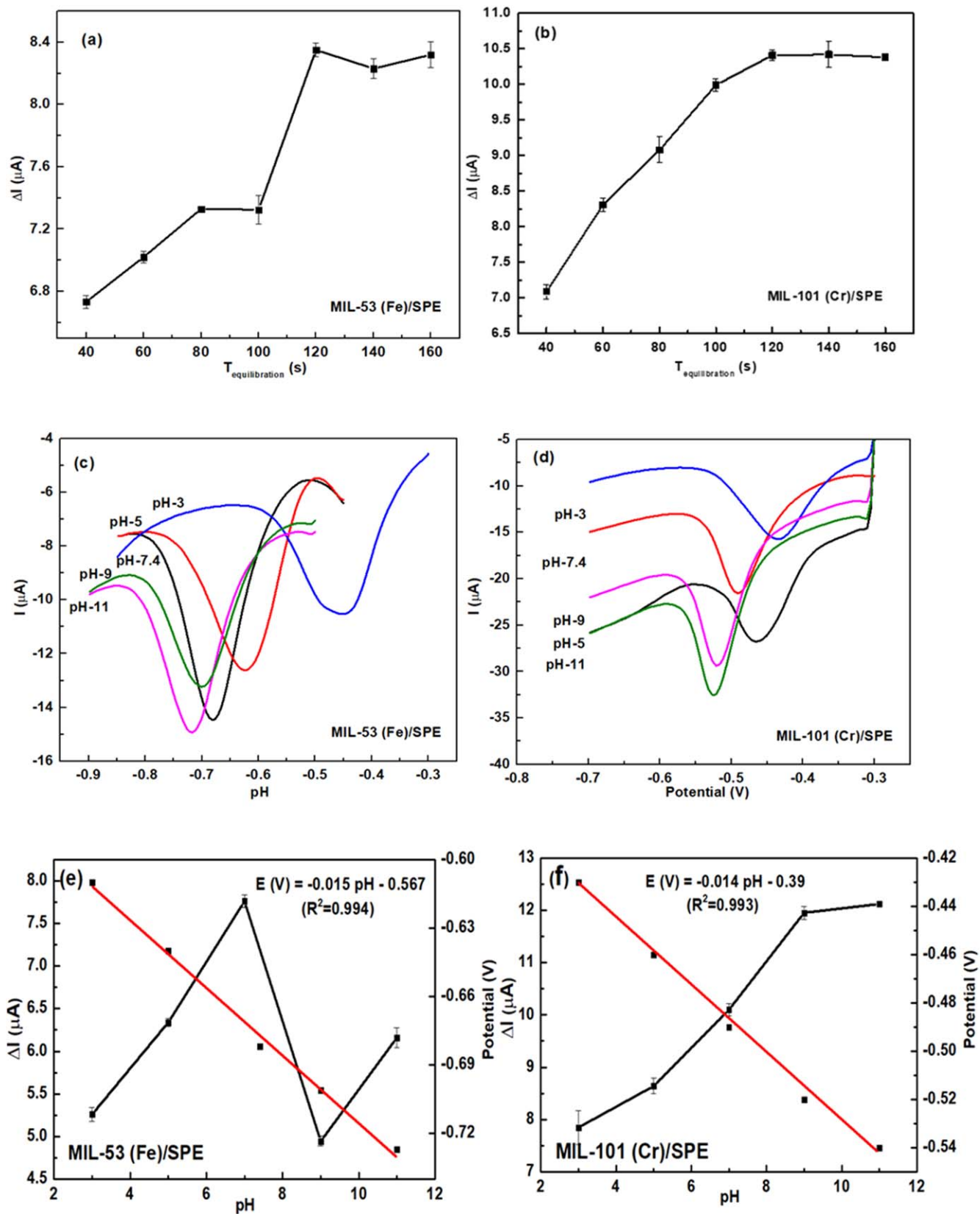
Figure 7. (a)–(d): the influence of $T_{equilibrium}$ and pH of 0.1 M PBS on current response of 50 μM CAP; (e) and (f): The variation of the reduction peak current and potential with pH at MIL-53(Fe)/SPE and MIL-101(Cr)/SPE.

possessed not only a huge surface area and large pore volume but also many strong electrocatalytic metal sites (Cr^{3+} ions). However, here it is limited by the steric effect due to small pore size, poor

adsorption and diffusion capacity due to the strong water-molecule interaction force of the metal centers. While, MIL-53(Fe) with a much smaller specific surface area and pore volume, it still showed a
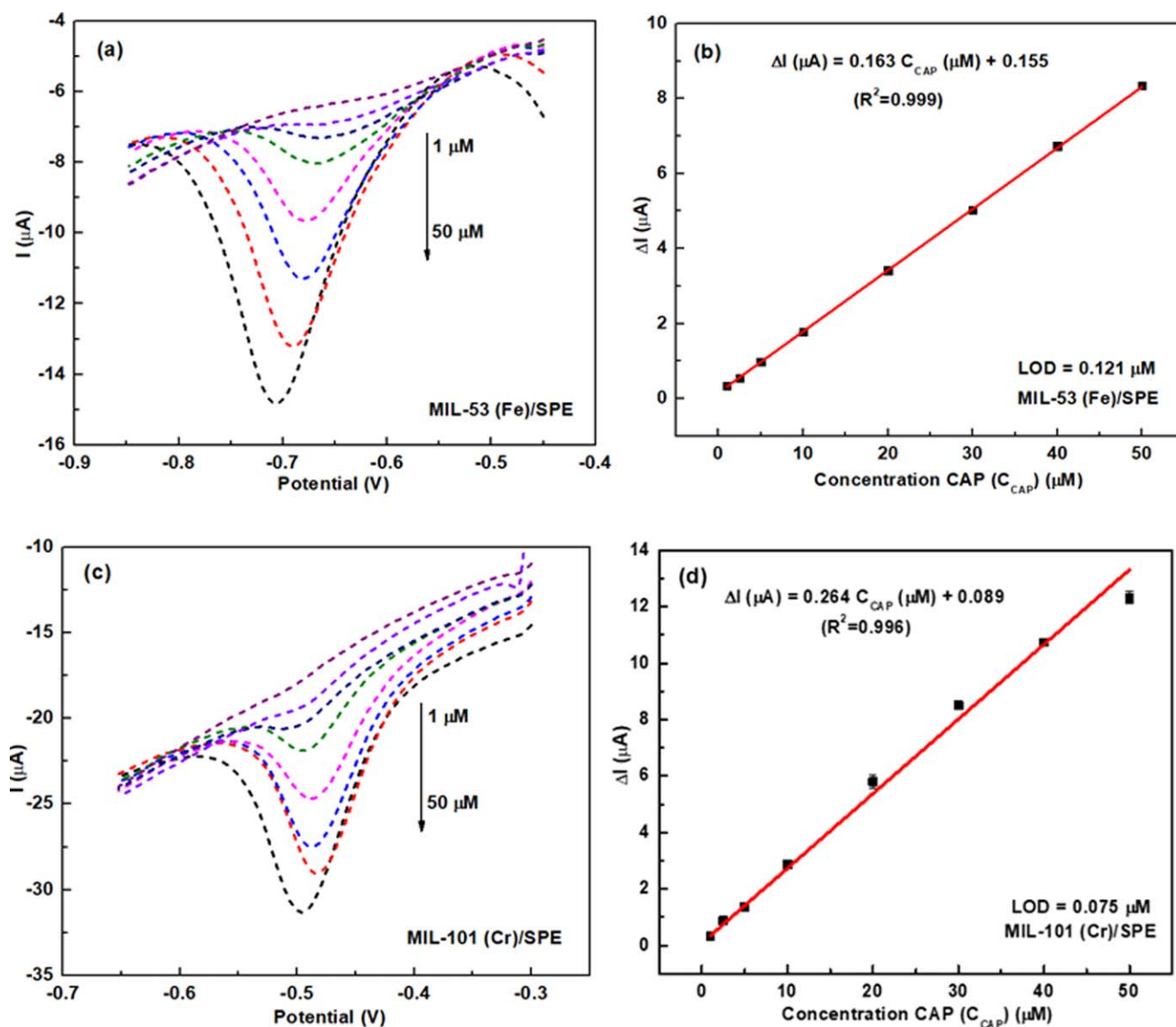
Figure 8. (a) and (c): DPV curves of CAP in the concentration range from 1 to 50 μM (pH = 7.4 and pH = 9) on MIL-53(Fe)/SPE and MIL-101(Cr)/SPE at a scan rate 6 mV s^{-1}, corresponding to the calibration plots between current intensity and concentration with error bars (b) and (d).

variety of electrocatalytic metal centers (Fe^{3+} ions) with high interaction ability and large adsorption capacity with CAP through hydrogen bonding and weak interaction with water molecules. As a result, the electrochemical performance of CAP on both two electrodes was almost similar in further electrochemical analyses. From the obtained results and detailed analysis, it can be seen that finding a balance between the conductivity and adsorption capacity as well as the electrocatalytic ability of MIL materials is extremely important in electrochemical sensor applications. A high potential MIL material in electrochemical sensors needs to meet in terms of both the conductivity, adsorption capacity, and electrocatalytic ability, which are strongly decided by the metal centers in the MIL structure.

Conclusions

In summary, the enhancement in electrochemical performance towards CAP detecting on MILs-modified electrodes has been elucidated. For MILs-modified electrodes, although their poor conductivity, the electrode modified with MIL-101(Cr)/SPE and MIL-53(Fe)/SPE still rendered them the better electrochemical performance of CAP through

the enhancement of the EASA, electrocatalytic ability, adsorption capacity, diffusion ability, and interact ability with the CAP molecules. Meanwhile, MIL-53(Al)/SPE showed a poor electrochemical response in the order of MIL-101(Cr)/SPE > MIL-53(Fe)/SPE ≫ MIL-53(Al)/ SPE > bare SPE. Indeed, MIL-101(Cr)/SPE and MIL-53(Fe)/SPE provided a rather wide linear concentration range from 1 to 50 μM along with low LOD values of about 0.121 and 0.075 μM (S/N = 3), respectively. Furthermore, the MILs-modified electrodes also exhibited good selectivity and high repeatability. Under an in-depth view, it can be seen that each material has its advantages and disadvantages suitable for particular applications. Understanding the nature of the material and the direction of the application will help us make the most of the advantages as well as inhibit disadvantages and come up with appropriate improvement solutions. In this case, MIL materials have semiconductor-like behaviors with weak conductivity, but they possess high adsorption capacity and outstanding electrocatalytic activity depending on metal centers. Therefore, finding a perfect balance between the electrical conductivity and adsorption capacity as well as the electrocatalytic ability of MIL materials is extremely important in electrochemical sensor applications. This study hopes to pave new development pathways for MIL materials in sensing applications.
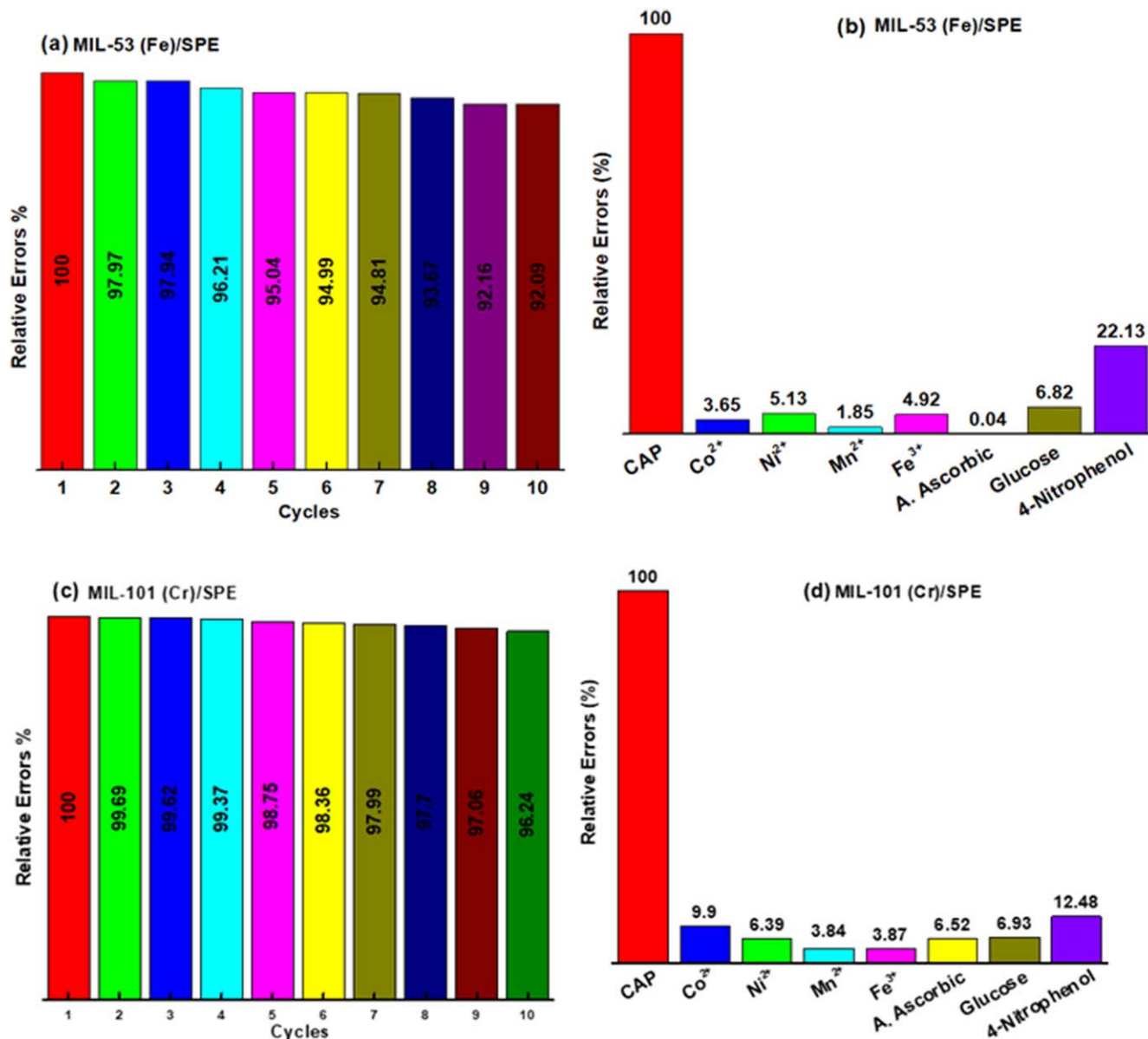
Figure 9. The repeatability and selectivity investigation of MIL-53(Fe)/SPE and MIL-101(Cr)/SPE using DPV technique.

ORCID

Tuyet Nhung Pham ⓘD https://orcid.org/0000-0003-1790-1457
Anh-Tuan Le ⓘD https://orcid.org/0000-0002-5648-3414

References

1. J. Imanipoor, M. Mohammadi, M. Dinari, and M. R. Ehsani, "Adsorption and desorption of amoxicillin antibiotic from water matrices using an effective and recyclable MIL-53(Al) metal–organic framework adsorbent." *J. Chem. Eng. Data*, **66**, 389 (2020).
2. T. Araya, M. Jia, J. Yang, P. Zhao, K. Cai, W. Ma, and Y. Huang, "Resin modified MIL-53 (Fe) MOF for improvement of photocatalytic performance." *Appl. Catal. B: Environ.*, **203**, 768 (2017).
3. X.-D. Do, V.-T. Hoang, and S. Kaliaguine, "MIL-53(Al) mesostructured metal-organic frameworks." *Microporous Mesoporous Mater.*, **141**, 135 (2011).
4. Y. R. Lee, K. Yu, S. Ravi, and W. S. Ahn, "Selective adsorption of rare earth elements over functionalized Cr-MIL-101." *ACS Appl. Mater. Interfaces*, **10**, 23918 (2018).
5. W. Xiong et al., "Adsorption of tetracycline antibiotics from aqueous solutions on nanocomposite multi-walled carbon nanotube functionalized MIL-53(Fe) as new adsorbent." *Sci. Total Environ.*, **627**, 235 (2018).
6. D. Cheng, X. Li, Y. Qiu, Q. Chen, J. Zhou, Y. Yang, Z. Xie, P. Liu, W. Cai, and C. Zhang, "A simple modified electrode based on MIL-53(Fe) for the highly sensitive detection of hydrogen peroxide and nitrite." *Anal. Methods*, **9**, 2082 (2017).
7. W. Cheng, X. Tang, Y. Zhang, D. Wu, and W. Yang, "Applications of metal-organic framework (MOF)-based sensors for food safety: Enhancing mechanisms and recent advances." *Trends Food Sci. Technol.*, **112**, 268 (2021).
8. R. Liang, L. Shen, F. Jing, N. Qin, and L. Wu, "Preparation of MIL-53(Fe)-reduced graphene oxide nanocomposites by a simple self-assembly strategy for increasing interfacial contact: efficient visible-light photocatalysts." *ACS Appl. Mater. Interfaces*, **7**, 9507 (2015).
9. S. Tajik, H. Beitollahi, F. Garkani Nejad, I. Sheikhshoaie, A. S. Nugraha, H. W. Jang, Y. Yamauchi, and M. Shokouhimehr, "Performance of metal–organic frameworks in the electrochemical sensing of environmental pollutants." *J. Mater. Chem. A*, **9**, 8195 (2021).
10. H. V. Tran, H. T. M. Dang, L. T. Tran, C. Van Tran, C. D. Huynh, and S. Roy, "Metal-organic framework MIL-53(Fe): synthesis, electrochemical characterization, and application in development of a novel and sensitive electrochemical sensor for detection of cadmium ions in aqueous solutions." *Adv. Polym. Technol.*, **2020**, 1 (2020).

11. C. Yue et al., "Study on the stability, evolution of physicochemical properties, and postsynthesis of metal-organic frameworks in bubbled aqueous ozone solution." *ACS Appl. Mater. Interfaces*, **13**, 26264 (2021).

12. Y. Li, C. Huangfu, H. Du, W. Liu, Y. Li, and J. Ye, "Electrochemical behavior of metal–organic framework MIL-101 modified carbon paste electrode: An excellent candidate for electroanalysis." *J. Electroanal. Chem.*, **709**, 65 (2013).

13. Z. Meng, M. Li, J. Shao, L. Yan, H. Yang, and X. Liu, "A sensitive electrochemical sensor based on the partial thermal decomposition of MIL-53(Fe) and reduced graphene oxide for phenol detection." *Ionics*, **27**, 4897 (2021).

14. W. Zhang, Z. Zhang, Y. Li, J. Chen, X. Li, Y. Zhang, and Y. Zhang, "Novel nanostructured MIL-101(Cr)/XC-72 modified electrode sensor: A highly sensitive and selective determination of chloramphenicol." *Sens. Actuators B: Chem.*, **247**, 756 (2017).

15. L. Zhang, X. Ma, H. Liang, H. Lin, and G. Zhao, "A non-enzymatic glucose sensor with enhanced anti-interference ability based on a MIL-53(NiFe) metal-organic framework." *J. Mater. Chem. B*, **7**, 7006 (2021).

16. L. Hamon, C. Serre, T. Devic, T. Loiseau, F. Millange, G. ´rard Fe´rey, and G. D. Weireld, "Comparative study of hydrogen sulfide adsorption in the MIL-53(Al, Cr, Fe), MIL-47(V), MIL-100(Cr), and MIL-101(Cr) metal-organic frameworks at room temperature." *J. Am. Chem. Soc.*, **131**, 8775 (2009).

17. L. Pukdeejorhor, K. Adpakpang, P. Ponchai, S. Wannapaiboon, S. Ittisanronnachai, M. Ogawa, S. Horike, and S. Bureekaew, "Polymorphism of mixed metal Cr/Fe terephthalate metal–organic frameworks utilizing a microwave synthetic method." *Cryst. Growth Des.*, **19**, 5581 (2019).

18. L. Hu, G. Deng, W. Lu, S. Pang, and X. Hu, "Deposition of CdS nanoparticles on MIL-53(Fe) metal-organic framework with enhanced photocatalytic degradation of RhB under visible light irradiation." *Appl. Surf. Sci.*, **410**, 401 (2017).

19. G. de Combarieu, M. Morcrette, F. Millange, N. Guillou, J. Cabana, C. P. Grey, I. Margiolaki, G. Fe´rey, and J.-M. Tarascon, "Influence of the Benzoquinone Sorption on the Structure and Electrochemical Performance of the MIL-53(Fe) Hybrid Porous Material in a Lithium-Ion Battery." *Chem. Mater.*, **21**, 1602 (2009).

20. Z. Noorpoor, S. G. Pakdehi, and A. Rashidi, "High capacity and energy-efficient dehydration of liquid fuel 2-dimethyl amino ethyl azide (DMAZ) over chromium terephthalic (MIL-101) nanoadsorbent." *Adsorption*, **23**, 743 (2017).

21. Ş. S. Bayazit, S. T. Danalıoğlu, M. Abdel Salam, and Ö. Kerkez Kuyumcu, "Preparation of magnetic MIL-101 (Cr) for efficient removal of ciprofloxacin." *Environ. Sci. Pollut. Res.*, **24**, 25452 (2017).

22. R. Liu, L. Chi, X. Wang, Y. Wang, Y. Sui, T. Xie, and H. Arandiyan, "Effective and selective adsorption of phosphate from aqueous solution via trivalent-metals-based amino-MIL-101 MOFs." *Chem. Eng. J.*, **357**, 159 (2019).

23. C. W. Ashling et al., "Synthesis and properties of a compositional series of MIL-53 (Al) metal–organic framework crystal-glass composites." *J. Am. Chem. Soc.*, **141**, 15641 (2019).

24. Z. Li, Y.-n Wu, J. Li, Y. Zhang, X. Zou, and F. Li, "The metal–organic framework MIL-53(Al) constructed from multiple metal sources: alumina, aluminum hydroxide, and boehmite." *Chem. Eur. J.*, **21**, 6913 (2015).

25. D. T. C. Nguyen et al., "Metal-organic framework MIL-53(Fe) as an adsorbent for ibuprofen drug removal from aqueous solutions: response surface modeling and optimization." *J. Chem.*, **2019**, 5602957 (2019).

26. Y. Zhang, G. Li, H. Lu, Q. Lv, and Z. Sun, "Synthesis, characterization and photocatalytic properties of MIL-53(Fe)–graphene hybrid materials." *RSC Adv.*, **4**, 7594 (2014).

27. B. Seoane, C. Téllez, J. Coronas, and C. Staudt, "NH₂-MIL-53(Al) and NH₂-MIL-101(Al) in sulfur-containing copolyimide mixed matrix membranes for gas separation." *Sep. Purif. Technol.*, **111**, 72 (2013).

28. H. Zhuang, W. Zhang, L. Wang, Y. Zhu, Y. Xi, and X. Lin, "Vapor deposition-prepared MIL-100(Cr)- and MIL-101(Cr)-supported iron catalysts for effectively removing organic pollutants from water." *ACS Omega*, **6**, 25311 (2021).

29. D. Wang, F. Jia, H. Wang, F. Chen, Y. Fang, W. Dong, G. Zeng, X. Li, Q. Yang, and X. Yuan, "Simultaneously efficient adsorption and photocatalytic degradation of tetracycline by Fe-based MOFs." *J. Colloid Interface Sci.*, **519**, 273 (2018).

30. E. Jangodaz, E. Alaie, A. A. Safekordi, and S. Tasharrofi, "Adsorption of ethylbenzene from air on metal–organic frameworks MIL-101(Cr) and MIL-53 (Fe) at room temperature." *J. Inorg. Organomet. Polym. Mater.*, **28**, 2090 (2018).

31. I. Streeter, G. G. Wildgoose, L. Shao, and R. G. Compton, "Cyclic voltammetry on electrode surfaces covered with porous layers: An analysis of electron transfer kinetics at single-walled carbon nanotube modified electrodes." *Sens. Actuators B: Chem.*, **133**, 462 (2008).

32. P. Krishnaveni and V. Ganesh, "Electron transfer studies of a conventional redox probe in human sweat and saliva bio-mimicking conditions." *Sci Rep.*, **11**, 7663 (2021).

33. Y. Li, J. Zhang, and H. Liu, "Removal of chloramphenicol from aqueous solution using low-cost activated carbon prepared from typha orientalis." *Water*, **10**, 351 (2018).

34. N. N. Tri, A. J. P. Carvalho, A. V. Dordio, M. T. Nguyen, and N. T. Trung, "Insight into the adsorption of chloramphenicol on a vermiculite surface." *Chem. Phys. Lett.*, **699**, 107 (2018).

35. J. W. Jun, M. Tong, B. K. Jung, Z. Hasan, C. Zhong, and S. H. Jhung, "Effect of central metal ions of analogous metal-organic frameworks on adsorption of organoarsenic compounds from water: plausible mechanism of adsorption and water purification." *Chem.*, **21**, 347 (2015).

36. M. N. Timofeeva, V. N. Panchenko, N. A. Khan, Z. Hasan, I. P. Prosvirin, S. V. Tsybulya, and S. H. Jhung, "Isostructural metal-carboxylates MIL-100(M) and MIL-53(M) (M: V, Al, Fe and Cr) as catalysts for condensation of glycerol with acetone." *Appl. Catal. A: Gen.*, **529**, 167 (2017).

37. E. Soubeyrand-Lenoir, C. Vagner, J. W. Yoon, P. Bazin, F. Ragon, Y. K. Hwang, C. Serre, J.-S. Chang, and P. L. Llewellyn, "How water fosters a remarkable 5-fold increase in low-pressure CO_2 uptake within mesoporous MIL-100(Fe)." *J. Am. Chem. Soc.*, **134**, 10174 (2012).

38. M. Tong, D. Liu, Q. Yang, S. Devautour-Vinot, G. Maurin, and C. Zhong, "Influence of framework metal ions on the dye capture behavior of MIL-100 (Fe, Cr) MOF type solids." *J. Mater. Chem. A*, **1**, 8534 (2013).